

Shot noise in low-dimensional systems

Massimo Macucci

Dipartimento di Ingegneria dell'Informazione: Elettronica, Informatica, Telecomunicazioni,
Università di Pisa

Paolo Marconcini

Dipartimento di Ingegneria dell'Informazione: Elettronica, Informatica, Telecomunicazioni,
Università di Pisa

Giuseppe Iannaccone

Dipartimento di Ingegneria dell'Informazione: Elettronica, Informatica, Telecomunicazioni,
Università di Pisa

Bruno Pellegrini

Dipartimento di Ingegneria dell'Informazione: Elettronica, Informatica, Telecomunicazioni,
Università di Pisa

Proceedings of the
17th International Conference

Noise and Fluctuations

August 18-22 2003,
Charles University Conference Centre
Prague, Czech Republic



ICNF 2003

PRAGUE

Editor

Josef Sikula

*Czech Noise Research Laboratory
Brno University of Technology*

SHOT NOISE IN LOW-DIMENSIONAL SYSTEMS

M. MACUCCI*, P. MARCONCINI, G. IANNACCONE, B. PELLEGRINI

Dipartimento di Ingegneria dell'Informazione

Via Diotisalvi, 2 I-56122 Pisa, Italy

**E-mail: macucci@mercurio.iet.unipi.it*

2. With an increase of p^2 , the coefficient which multiplies the nonlinear term, the right bifurcation occurs at larger amplitude E , and the jump becomes larger.
3. With an increase of b (and c) which describe the parametric excitation the left bifurcation occurs at somewhat larger amplitude E , and the jump becomes slightly larger.
4. For not too large coefficients b (and c) the amplitude of the output signal A vanishes at some value of the amplitude E of a low frequency field.

We look forward for experimental verification of these predictions.

References

- [1] R. Benzi, S. Sutera, and A. Vulpiani, The mechanism of stochastic resonance, *J. Phys. A* (1981) **14**, L453 - L457.
- [2] L. Gammaitoni, P. Hanggi, P. Jung, and F. Marchesoni, Stochastic resonance, *Rev. Mod. Phys.* **70** (1998) 223 - 287.
- [3] M. I. Tsindlekht, I. Felner, M. Gitterman, and B. Ya. Shapiro, Stochastic resonance phenomenon in a superconducting surface state of single-crystal Nb, *Phys. Rev.* **62** (2000) 4073-4078.
- [4] R. W. Rollins and J. Silcox, Nature of ac transition in superconducting surface sheath in Pb - 2% on, *Phys. Rev.* **155** (1967) 404 - 418.
- [5] B. McNamara and K. Wiesenfeld, *Phys. Rev. A* **39** (1989) 4854 - 4869.
- [6] V. Berdichevsky and M. Gitterman, Influence of a periodic field on two-level classical systems, *Phys. Rev. E* **59** (1999) R9-R11.
- [7] M. I. Tsindlekht, I. Felner, and G. Jung, Giant non-linear response of superconducting single crystal niobium in a sweeping magnetic field, *Physica C* **372-376** (2002) 1827 - 1829.

We present numerical simulations of shot noise suppression in low-dimensional systems, focusing on the different limiting values of the Fano factor (ratio of the current noise power spectral density to the full shot noise power spectral density) for specific structures such as diffusive conductors, regular antidot lattices, chaotic cavities. We also study the dependence of the Fano factor for a chaotic cavity on magnetic field, proposing an intuitive explanation for the results, based on the ratio of the classical cyclotron radius to the width of the apertures defining the cavity.

1. Introduction

Low-dimensional structures offer unique opportunities for the investigation of shot noise suppression and enhancement effects, due to the presence of a limited number of transmitted modes and of Coulomb and Pauli exclusion phenomena. In the last decade several theoretical papers have been published, predicting “universal” shot noise suppression factors for specific structures: Beenakker and Büttiker have shown [1], using Random Matrix Theory (RMT), that shot noise is suppressed down to 1/3 of its full value in diffusive conductors, the same result has then been obtained with a semiclassical approach including the Pauli exclusion principle by Nagaev [2]; Jalabert *et al.* [3] have shown that shot noise in a symmetric chaotic cavity is reduced down to 1/4 of its full value using RMT, while Blanter and Sukhorukov [4] have reached the same result with a semiclassical treatment. The 1/3 suppression has been experimentally demonstrated in diffusive metallic conductors by Henny *et al.* [5] and the suppression factor 1/4 for chaotic cavities has been experimentally confirmed, too, by Oberholzer *et al.* [6]. Random Matrix Theory and semiclassical approaches are powerful methods that allow a compact analytical or semi-analytical treatment of rather complex problems, but are not directly applicable to generic geometries and do not allow straightforward inclusion of the effects of a magnetic field. We have developed numerical techniques that allow computing the low-frequency shot noise power spectral density in generic nanostructures and that are particularly suitable to treat relatively large devices, such as the chaotic cavities.

2. Numerical Methods

The main aim of the calculations is that of obtaining the transmission matrix for the whole structure, from which the conductance and the low-frequency noise power spectral density can be derived with a simple procedure that will be described in the following. In the case of no magnetic field ($B = 0$), we use an approach based on the recursive combination of Green's functions: the device is subdivided into a number of transverse slices, which are thin enough as to justify the assumption that within each of them there is no significant variation of the transverse confinement potential along the longitudinal direction. Each

slice is initially considered isolated from its neighbors and with Dirichlet boundary conditions at its ends [7], so that its Green's function can be obtained analytically, in the form of a diagonal matrix, if we use a mixed representation, over the transverse eigenmodes in the transverse direction and in real space in the longitudinal direction. Using the Dyson equation it is possible [8] to compute the overall Green's function matrix for two adjacent coupled slices, starting from their individual Green's functions. Thus we start computing the Green's function for the two rightmost slices and then move backward recursively, adding one slice at a time, until we have obtained the Green's function for the global, connected structure. The first and last slice are not actually finite-length slices, but, instead, semi-infinite leads that allow the introduction of open boundary conditions [8]. From the overall Green's function matrix of the structure, the transmission matrix t' can be derived with a straightforward procedure detailed in Ref. [7].

For the calculations in which a magnetic field perpendicular to the plane of the structure is included, we have used a recursive scattering matrix technique. We assume that the nanostructure lies in the x, y plane, with x being the propagation direction and we choose the transverse gauge corresponding to a vector potential with a nonzero component only along x . In each of the M slices into which the structure has been subdivided, based on the same criteria that we have already examined for the Green's function technique, the electron wave function can be written in terms of products of right-going and left-going plane waves times transverse wave functions expandable over a basis of transverse eigenfunctions for $B = 0$. The coefficients of such an expansion can be determined following the procedure outlined by Tamura and Ando, i.e. by solving a properly constructed eigenvalue problem [9], which yields also the longitudinal eigenvectors.

Once the longitudinal wave vectors and the transverse wave functions in each of the mentioned slices have been computed, we use the mode-matching technique to obtain the scattering matrix of the $M - 1$ sections assembled joining adjacent half slices (therefore each of them includes one discontinuity of the potential energy in the x direction)

Then, combining recursively the $M - 1$ scattering matrices, we obtain the scattering matrix of the overall structure, from which we extract the transmission matrix t' , including only the propagating modes and normalizing its elements with respect to the probability currents.

Let us now see how the conductance and low-frequency noise power spectral density can be computed from t' . We apply the Landauer formula for the evaluation of the conductance, obtaining

$$G = \frac{2e^2}{h} \sum_{n,m} |t'_{nm}|^2 \quad (1)$$

while we derive the noise power spectral density following Büttiker's approach [10],

$$S_I = 4 \frac{e^3}{h} |V| \sum_j w_j (1 - w_j), \quad (2)$$

where w_j are the eigenvalues of the matrix $t' t'^{\dagger}$ and V is the bias voltage externally applied to the structure. Since the full shot noise power spectral density is given by $2e|I| = 2e|V|G$, the Fano factor γ reads

$$\gamma = \frac{\sum_j w_j (1 - w_j)}{\sum_{n,m} |t'_{nm}|^2}. \quad (3)$$

3. Shot Noise in Diffusive Conductors

We represent a diffusive mesoscopic conductor by including a number of hard-wall, randomly distributed scatterers in a quantum wire. In order to achieve the diffusive regime, a specific relationship must exist between the length L of the device, the elastic mean free path l and the number of propagating modes N . Such a relationship is described by the inequality $l \ll L \ll Nl$. It is therefore apparent that the device must be longer than the inelastic mean free path and that N must be large, which poses severe problems from the computational point of view, and has required specific optimization of our Green's function code with respect to early approaches [11]. In Fig. 1 we report the Fano factor as a function of the Fermi energy for three structures that are $5 \mu\text{m}$ wide: curves are vertically shifted by 1 and the thin lines represent the value $1/3$. Starting from the top, we have results for a device $7.72 \mu\text{m}$ long with 600 square $25 \times 25 \text{ nm}^2$ scatterers, then for a device $3.86 \mu\text{m}$ long with 600 square $25 \times 25 \text{ nm}^2$ scatterers and, finally, for a structure $7.72 \mu\text{m}$ long with 600 square $12.5 \times 12.5 \text{ nm}^2$ obstacles. We notice that, with increasing Fermi energy and therefore with an increasing number of propagating modes, all curves converge to the value $1/3$. An estimate of the elastic mean free path can be obtained from the information we have about the conductance and the Drude model: if we compute l for the three cases, we notice that the $1/3$ limit is reached as soon as the number of propagating modes is such that $Nl > 3L$. If, instead of a random distribution of scatterers, we consider a regular

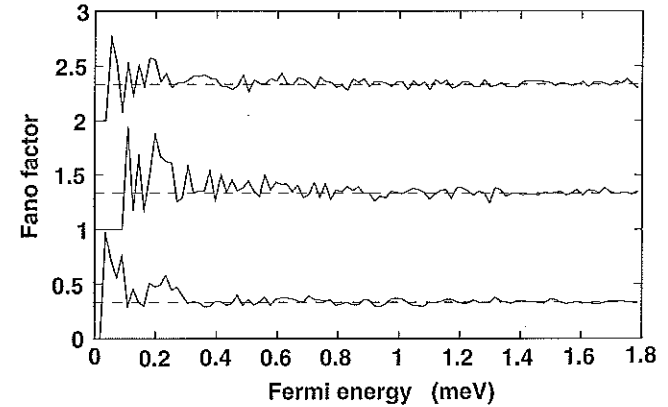


Fig. 1. Fano factor as a function of Fermi energy for a device $7.72 \mu\text{m}$ long with 600 square $25 \times 25 \text{ nm}^2$ scatterers (top curve), a device $3.86 \mu\text{m}$ long with 600 square $25 \times 25 \text{ nm}^2$ scatterers (middle curve), and a device $7.72 \mu\text{m}$ long with 600 square $12.5 \times 12.5 \text{ nm}^2$ scatterers (bottom curve).

arrangement, such as a square lattice of antidots, an interesting change in the Fano factor is observed: the Fano factor settles around a limiting value that depends on the antidot density and is well below $1/3$. In Fig. 2 we report with a solid line the results for the Fano factor as a function of the Fermi energy that we have obtained for a quantum wire $1.2 \mu\text{m}$ wide filled with $24 \times 24 \text{ nm}^2$ scatterers arranged in a square lattice with a separation of 220 nm . The dashed line represents instead the results for larger $48 \times 48 \text{ nm}^2$ scatterers arranged in a square 200 nm lattice. We notice that while the Fano factor for the smaller antidots settles around the value 0.11 , that for the larger antidots settles around 0.14 . Further increase of the antidot size does not lead to a significant increase in the limiting value

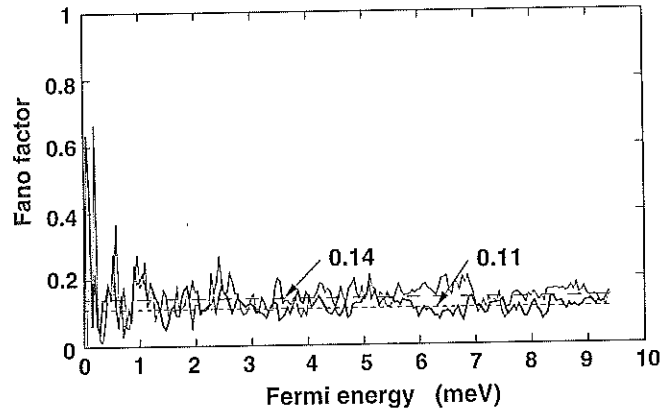


Fig. 2. Fano factor as a function of Fermi energy for square antidot lattices filling a quantum wire $1.2 \mu\text{m}$ wide: the thick curve is for $24 \times 24 \text{ nm}^2$ antidots with a separation of 220 nm and the thin curve is for $48 \times 48 \text{ nm}^2$ antidots with a separation of 200 nm .

of the Fano factor (which, for a square lattice, reaches at most $0.15 \div 0.16$), since bigger dots also mean less spacing between adjacent layers of dots in the longitudinal direction, which tends to reduce the noise [12], because in the limit of adjacent dots touching each other, continuous channels would be obtained, leading to a complete suppression of shot noise. Higher values of the Fano factor can be achieved only with a rectangular lattice in which the distance between antidots in the transverse direction is much smaller than that along the longitudinal direction. In this case the equivalent of cascaded chaotic cavities is obtained [12], and the Fano factor reaches the value 0.25.

4. Shot Noise in Chaotic Cavities

We have then analyzed the behavior of the Fano factor in a chaotic cavity $5 \mu\text{m}$ long and $8 \mu\text{m}$ wide as a function of the magnetic field. Since the results are affected by fluctuations, due to the complex interference patterns that arise inside the cavity, we have taken an average over the values of the Fano factor obtained in an energy interval with a width of 0.48 meV centered around the value of the Fermi energy of 9.14 meV that is reported for the experimental sample on which Oberholzer *et al.* have performed their measurements. We show in Fig. 3 the results for entrance and exit apertures with a width of 200 nm (solid dots), 100 nm (empty dots), 60 nm (empty squares) and 40 nm (solid squares). The experimental data of Ref. [13] have the same linear dependence of the Fano factor on the magnetic field as the results of our simulations.

We provide an intuitive explanation of this behavior alternative to that proposed by Oberholzer *et al.* and based on the analysis of the ratio of the classical cyclotron radius of the electron to the width of the apertures defining the cavity. In a magnetic field skipping orbits are formed with a radius corresponding to the cyclotron radius $R_c = \sqrt{2m^* E_f / (eB)}$, where m^* is the effective mass of the electron, E_f is the Fermi level. If the cyclotron radius becomes comparable to the width of the constrictions delimiting the cavity, the edge states will crawl through the constrictions and along the cavity perimeter,

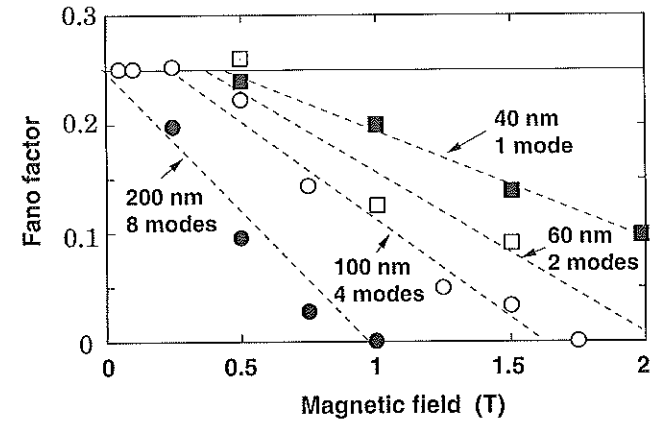


Fig. 3. Fano factor as a function of magnetic field in a chaotic cavity with apertures 200 nm wide (solid dots), 100 nm wide (empty dots), 60 nm wide (empty squares) and 40 nm wide (solid squares).

exiting the cavity with little or no probability of backscattering at the exit aperture. Therefore, as the magnetic field increases, the chaotic nature of transport gradually disappears, as edge states become more likely to allow traversal of the cavity without internal reflections, and shot noise is suppressed. The results shown in Fig. 3 are consistent with this interpretation: R_c for $B = 1 \text{ T}$ is 83.4 nm , which is definitely less than 200 nm , but only slightly less than 100 nm . Indeed, for $W = 200 \text{ nm}$ at 1 T noise appears to be completely suppressed, while for $W = 100 \text{ nm}$ suppression is not complete, with a Fano factor around 0.1.

5. Conclusions

Our simulation codes have been specifically optimized to deal with situations in which a very large number of propagating modes must be considered and have therefore allowed the analysis of shot noise suppression in diffusive conductors, in antidot lattices and in chaotic cavities with hundreds of modes participating in the conduction. In particular, we have been able to provide an estimate of the number of propagating modes needed to reach the diffusive regime in terms of the device length and of the elastic mean free path. As far as antidot lattices are concerned, we have shown that for square lattices a maximum Fano factor of $0.15 \div 0.16$ can be reached, while with a rectangular lattice it is possible to reach the value 0.25. Finally, we have reproduced with our simulations the experimental results that can be found in the recent literature on the dependence of the Fano factor on the magnetic field, proposing a simple and intuitive explanation based on the ratio of the cyclotron radius to the width of the constrictions defining the cavity.

Acknowledgments

This work has been supported by the Italian CNR (National Research Council) through the "5% Nanotechnology" program and by the University of Pisa.

References

- [1] C. W. J. Beenakker and M. Büttiker, Phys. Rev. B **46** (1992) 1889.
- [2] K. E. Nagaev, Phys. Lett. A **169** (1992) 103.
- [3] R. A. Jalabert, J.-L. Pichard, C. W. J. Beenakker, Europhys. Lett. **27** (1994) 255.
- [4] Ya. M. Blanter, E. V. Sukhorukov, Phys. Rev. Lett. **84** (2000) 1280.
- [5] M. Henny, S. Oberholzer, C. Strunk, and C. Schönberger, Phys. Rev. B **59** (1999) 2871.
- [6] S. Oberholzer, E. V. Sukhorukov, C. Strunk, C. Schönberger, T. Heinzel, M. Holland, Phys. Rev. Lett. **86** (2001) 2114.
- [7] F. Sols, M. Macucci, U. Ravaioli and Karl Hess, J. Appl. Phys. **66**, (1992) 3892.
- [8] M. Macucci, A. Galick, and U. Ravaioli, Phys. Rev. B **52**, (1995) 5210.
- [9] H. Tamura and T. Ando, Phys. Rev. B **44** (1991) 1792.
- [10] M. Büttiker, Phys. Rev. Lett. **65** (1990), 2901.
- [11] M. Macucci, G. Iannaccone, B. Pellegrini, in the Proceedings of the 15th International Conference on Noise in Physical Systems and $1/f$ Fluctuations, Hong Kong, (Aug. 1999) 325.
- [12] M. Macucci, Physica B **314** (2002) 494.
- [13] S. Oberholzer, E. V. Sukhorukov, C. Schönberger, Nature **415** (2002) 765.

CONCURRENT EFFECTS OF PAULI AND COULOMB INTERACTION IN RESONANT TUNNELING DIODES AT LOW BIAS AND LOW TEMPERATURE

G. IANNAACONE*, M. MACUCCI, G. BASSO, B. PELLEGRINI

Dipartimento di Ingegneria dell'Informazione, Università degli Studi di Pisa,

Via Diotisalvi, 2 I-56122 Pisa, Italy

**E-mail: g.iannaccone@iet.unipi.it*

In this talk we present a model for the physical simulation of noise in resonant tunneling diodes, based on the self-consistent solution of the Poisson-Schrödinger equation in one dimension. We focus on suppression of shot noise at low bias, as a concurrent effect of Pauli exclusion and Coulomb interaction, and show that such effect may be observable even at 77 K in a thin barrier AlGaAs-GaAs resonant tunneling diode, that we are presently investigating also from the experimental point of view.

1. Introduction

Deviations of the power spectral density of shot noise with respect to the value associated to a Poisson process have been investigated in several device structures and operating conditions. Such deviations are extremely interesting, since they are in most cases due to electron-electron interaction, of which they can represent a very sensitive probe.

Electrons typically interact through the electrostatic force and through Pauli exclusion, which tend to broaden the distribution of electrons in the phase space. Depending on the device structure and on the operating conditions, such interactions may alter the statistical properties of current fluctuations with respect to the case of non interacting electrons, in a way that is intimately related to the microscopic transport mechanisms.

When electrons are non-interacting, the transport process is Poissonian, and the power spectral density of the noise current is $S_{full} = 2qI$, where q is the electron charge, and I is the DC current through the device. The Fano factor, defined as the ratio of the power spectral density of the noise current to S_{full} , is the most used parameter for measuring the deviations with respect to a Poisson process. A broad review of many cases observed in the last ten years of noise literature can be found in Ref. [1].

In this talk, we want to describe the concurrent effects of Coulomb and Pauli interactions in a resonant tunneling diode at low bias and low temperature. The effect has been first predicted in Ref. [2], and has been studied from the analytical point of view in Ref. [3], but has not yet been observed in experiments, given the very low bias current and associated low differential conductance. Here, we consider a device with much thinner barriers with respect to those considered in Ref. [2], in order to verify whether the effect is still present in a device with higher differential conductance at low bias, and therefore easier to characterize at those regimes.

2. Model and Discussion

In order to investigate from a quantitative point of view such effects, we have developed a self-consistent 1D Poisson-Schrödinger solver which allows us to simulate DC and noise properties of resonant tunneling diodes. We shall refer to a particular structure, that we are presently investigating from the experimental point of view: it is an AlGaAs-GaAs double